

Tunable excitation spectrum in quantum double models

Anna Kómár¹ and Olivier Landon-Cardinal^{2,3}

¹*Institute for Quantum Information and Matter and Walter Burke Institute for Theoretical Physics, California Institute of Technology, Pasadena, California 91125, USA*

²*Département de Physique, McGill University, Montréal, Québec, Canada H3A 2T8*

³*Collège Jean-de-Brébeuf, Montréal, Québec, Canada H3T 1C1*

Kitaev's quantum double models, including the toric code, are canonical examples of quantum topological models on a 2D spin lattice. Their Hamiltonian define the groundspace by imposing an energy penalty to any nontrivial flux or charge, but treats any such violation in the same way. Thus, their energy spectrum is very simple. We introduce a new family of quantum double Hamiltonians with adjustable coupling constants that allow us to tune the energy of anyons while conserving the same groundspace as Kitaev's original construction. Those Hamiltonians are made of commuting four-body projectors that provide an intricate splitting of the Hilbert space.

I. INTRODUCTION

Interacting topological spin models are of interest in the field of condensed matter theory and quantum information due to their promising properties to encode quantum information into their degenerate groundspace. The different ground states can be labelled through a topological property of the system, e.g., by the equivalence classes of the different non-contractible loops on a torus. The quantum information encoded into a ground state can be recovered after a long time provided only local coherent errors are introduced by the environment. Thus, topological systems are inherently robust to decoherence.

One of the first proposals for a topological quantum code is the *toric code* by Kitaev [1]. This is a two-dimensional system with periodic boundary conditions, i.e., with a toroidal geometry, where physical spin-1/2 particles or *qubits* live on edges of a 2D square lattice. This model has a four-fold degenerate groundspace, i.e., the groundspace encodes two logical qubits. Any local operator acts trivially within the groundspace whereas operators acting on a large number of qubits residing on a noncontractible loop going around the torus act non-trivially. An experimentally more feasible version of the toric code is the *surface code* [2, 3], which is a two-dimensional system with physical qubits still placed on edges of a lattice, but the boundaries are now open: when excitations reach a boundary, they condense. Several experimental groups currently pursue the physical realization of surface codes [4, 5] with the goal to use them as building blocks in a quantum computer.

The toric code belongs to a more general class of topological systems known as *quantum doubles*, introduced by Kitaev [1] as a way to realize the mathematical construction [6] known as the Drinfeld double $\mathcal{D}(G)$ of a group G unto a spin lattice. For instance, the toric code is the quantum double $\mathcal{D}(\mathbb{Z}_2)$ based on the group \mathbb{Z}_2 .

The excitations of a quantum double are indistinguishable quasi-particles called anyons: *abelian* if taking anyons around each other modifies their wave function by only a phase, and *non-abelian* if taking certain anyons

around one another applies a nontrivial unitary operation to their wave function. In quantum double models, anyons carry a (nontrivial) charge or flux and are accordingly grouped into *chargeons*, *fluxons* and *dyons* when they carry both a (nontrivial) charge and a (nontrivial) flux.

Kitaev introduced quantum doubles by writing down a Hamiltonian whose groundspace is spanned by vacuum states, i.e., states with no flux nor charge present. More precisely, the Hamiltonian imposes an energy penalty equal to the number of nontrivial charge or flux present. Since different charges and fluxes are treated equally, the energy landscape of Kitaev quantum double Hamiltonian is very simple: all chargeons and fluxons have mass 1 and all dyons have mass 2 (in the correct energy units).

Enriching the energy landscape of a quantum double would modify its dynamics. Not only changing the Hamiltonian would modify its coherent dynamics but also its incoherent dynamics, for instance in the presence of a thermal environment. Engineering the Hamiltonian can result into interesting regimes, favorable to encoding quantum information. For instance, tuning the masses of excitations in abelian quantum doubles results in changed dynamics of the thermal processes [7], even if only in a restricted temperature regime [8]. However, to our knowledge, it was not known how to assign different masses to different anyons for non-abelian quantum doubles. The major obstacle was to account for dyons for which flux and charge do not decouple but rather combine in an intricate way.

In this paper, we introduce a Hamiltonian that assigns different masses to different anyons of non-abelian quantum doubles $\mathcal{D}(G)$. In such as *tunable mass Hamiltonian*, each term only acts on four neighboring higher-dimensional spin or qudits. Moreover, each 4-local terms commute pairwise, resulting in Hamiltonian which can be solved explicitly. We show how the 4-local charge and flux projectors assign different masses to anyons (including dyons) by partitioning the Hilbert space of anyons according to simple charge and flux labels related to the representation theory of the group G . The tunable parameters are the coupling constants for each 4-local term

which can be used to tune the anyon masses.

Throughout the paper, we illustrate the notions we introduced by analyzing the quantum double for the smallest non-Abelian group S_3 , the symmetry group of order 3, whose quantum double structure was explored in [9, 10]. We explicitly write down the 4-local tunable mass Hamiltonian for this theory, see Eq. (74).

The paper is organized as follows. First, in Sec. II we review the most important properties of non-abelian anyons, and introduce the quantum double construction. Second, in Sec. III we introduce the general charge and flux projectors and construct the 4-local tunable mass Hamiltonian. Theorem 8 is the main result of our paper. Third, we analyze how the qudit Hilbert space becomes partitioned through these projectors and introduce a diagrammatic representation to visualize this partitioning, see Fig. 8. Finally, we conclude our findings and point out future directions in Sec. V.

II. THE QUANTUM/DRINFELD DOUBLE CONSTRUCTION

The quantum double construction realizes topological lattice spin models whose anyonic excitations are described mathematically by the Drinfeld double of a group. To better appreciate the quantum double construction, we first review the properties and mathematical formalism of non-abelian anyons in general. First, in Sec. II A we give an overview of the anyon labels and the most important braiding properties. This pedagogical exposition is largely inspired from John Preskill's lecture notes [11] and the reader is encouraged to consult those notes for more details. We finally introduce the quantum double construction on a lattice in Sec. II B.

A. Non-Abelian Aharonov-Bohm effect

Anyons can be understood by analogy to the Aharonov-Bohm effect: taking a charge q around a flux tube with flux Φ results in the wave function acquiring a phase $\exp(iq\Phi)$.

$$|\psi\rangle \rightarrow \exp(iq\Phi)|\psi\rangle \quad (1)$$

Non-Abelian anyons can be qualitatively understood by generalizing the Aharonov-Bohm effect to fluxes whose possible values correspond to the elements g of a group G and the charge possible values are the irreducible representations (irreps) Γ of G . In other words, the Hilbert space of each quasiparticle is spanned either by the flux orthonormal basis

$$\mathcal{H} = \text{span}\{|g\rangle\}_{g \in G}. \quad (2)$$

or in a conjugate charge orthonormal basis

$$\mathcal{H} = \text{span}\{|\Gamma, i\rangle\}_{\text{irrep } \Gamma, i=1 \dots |\Gamma|} \quad (3)$$

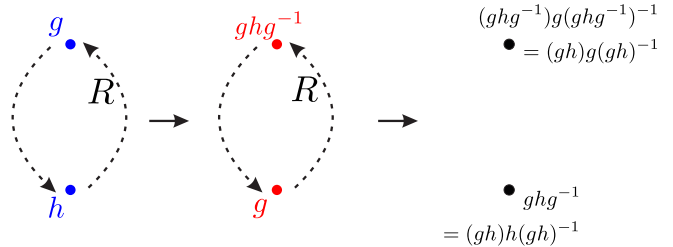


Figure 1. Braiding of two anyons, g and h : applying a counterclockwise exchange of the particles, resulting in conjugacy of the original wave function.

in which we chose an (arbitrary) orthonormal basis $\{|\Gamma, i\rangle_{i=1 \dots |\Gamma|}\}$ for every module of each irrep Γ .

1. Labelling fluxons

To identify a fluxon, we can check how the basis transforms when a charge Γ is transported around the fluxon

$$|\Gamma, j\rangle \rightarrow \sum_{i=1}^{|\Gamma|} D_{ij}^{\Gamma}(a)|\Gamma, i\rangle \quad (4)$$

Since the matrix elements $D_{ij}^{\Gamma}(a)$ can in principle be measured by interferometry [12], performing this for every charge type $|\Gamma, j\rangle$ will reveal the flux $a \in G$.

However, labelling fluxons by group elements is not gauge-invariant since another observer could choose another orthonormal basis for the module of the irrep Γ . In fact, the correct gauge-invariant quantity to label fluxons is the *conjugacy class*:

Definition 1 (Conjugacy class).

$$C_a = \{gag^{-1} | g \in G\}. \quad (5)$$

Indeed, two observers will agree on the conjugacy class of a fluxon even if they probably would disagree on the representative group element within the conjugacy class.

2. Braiding of fluxons

We now want to understand what happens when braiding fluxons. Let's consider two fluxons side by side. The top fluxon has flux a while the bottom fluxon has flux b (locally, flux types are well defined). Let's now counter-clockwise exchange the fluxons, resulting in an operator R_{ab} . One can prove that the resulting effect is

$$R_{ab} : |a, b\rangle \mapsto |aba^{-1}, a\rangle \quad (6)$$

i.e., the top flux has been conjugated by the bottom flux. See Fig. 1 for a pictorial representation.

Note that two successive counterclockwise exchange is equivalent to having the rightmost flux going around the leftmost flux counterclockwise, see Fig. 1. The net result of that operation is

$$R_{ab}^2 : |a, b\rangle \mapsto |(ab)a(ab)^{-1}, (ab)b(ab)^{-1}\rangle \quad (7)$$

which is coherent with the claim that the conjugacy class of a fluxon is gauge-invariant but the representative is ambiguous since it can change by an arbitrarily far away fluxon moving around it.

3. Total flux/charge of a pair of fluxons

A key feature of anyon models is that some physical properties are non-local. One such property is the total flux of a pair of fluxons. For instance, a pair of fluxons can have a trivial total flux. In that case, we expect that the global effect of a double counterclockwise exchange should be trivial. This occurs if $ab = e$ where e is the identity element of the group. However, for pair of fluxons $|a, b\rangle$ where $ab \neq e$, the total flux can be non-trivial.

Let's consider two fluxons whose total flux is trivial, i.e., a state $|a, a^{-1}\rangle$. One would be tempted to think that those two fluxons arose from the vacuum. However, this is not necessarily the case since this pair of fluxons can carry charge! Indeed, in order to identify the charge of the pair, let's carry a test fluxon b around the pair. In the reference frame of the test fluxon b , the pair of fluxons is transported around the test fluxon. In other words, a (potentially) charged object is carried around a test fluxon. Then, one can identify the charge by interferometry, like in Eq. (4). Thus, this local measurement will reveal the total charge of the pair of fluxons. However, this physical property would be highly non-local if the two fluxons were spatially separated. Nonetheless, their total charge would be well defined!

4. Transferring charge from a chargeon to a fluxon

We will now consider another topological feature: the transfer of charge from a chargeon to a fluxon through braiding.

Let $|0, C_g\rangle$ be a state of two fluxons of the conjugacy class C_g whose total flux is trivial and whose total charge is trivial. One can prove that

$$|0, C_g\rangle = \frac{1}{\sqrt{|C_g|}} \sum_{a \in C_g} |a, a^{-1}\rangle \quad (8)$$

That pair of fluxons can be created out of the vacuum since they globally carry trivial charge and trivial flux.

Similarly, let $|0, \Gamma\rangle$ be a state of two chargeons carrying individually a non-trivial charge whose total flux is trivial and whose total charge is trivial. If one chargeon carries the charge corresponding to irrep Γ , there exists a unique

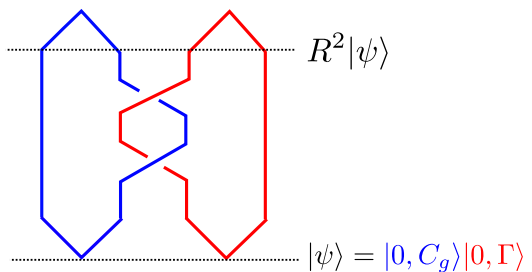


Figure 2. Braiding diagram corresponding to the transfer of a charge from a chargeon (in red) to a fluxon (in blue).

representation $\bar{\Gamma}$ that can be combined to Γ to give the trivial representation. If $\{|\Gamma, i\rangle\}$ is a basis for Γ , we can choose a basis $\{|\bar{\Gamma}, i\rangle\}$ for the conjugate representation $\bar{\Gamma}$ such that the state of the two chargeons is

$$|0, \Gamma\rangle = \frac{1}{\sqrt{|\Gamma|}} \sum_i |\Gamma, i\rangle \otimes |\bar{\Gamma}, i\rangle \quad (9)$$

That pair of chargeons can be created out of the vacuum since it the pair has trivial charge and trivial flux.

Suppose we create this pair of fluxons and this pair of chargeons out of the vacuum. The resulting state is

$$|\psi\rangle = |0, C_g\rangle \otimes |0, \Gamma\rangle \quad (10)$$

Suppose we now perform a double-counterclockwise-exchange R^2 of the chargeon carrying charge Γ with one of the fluxon. This corresponds to the braiding diagram on Fig. 2.

The resulting entangled state is

$$R^2|\psi\rangle = \frac{1}{\sqrt{|\Gamma|}} \frac{1}{\sqrt{|C_g|}} \sum_{x \in C_g} |x, x^{-1}\rangle \sum_{ij} D_{ij}^\Gamma(x) |\Gamma, i\rangle \otimes |\bar{\Gamma}, j\rangle \quad (11)$$

where $\{D_{ij}^\Gamma(x)\}_{ij}$ is the matrix representing element x in the irrep Γ .

Suppose we now try to fuse the braided chargeon with its original partner and the braided fluxon with its original partner. Naively, one could think that the braiding has no effect and that the total charge (resp. flux) of the chargeons (resp. fluxons) is trivial. We will see that this is not the case, which can be interpreted as a transfer of charge from the chargeon to the fluxon. Indeed, the probability of fusing back to the vacuum after the double-exchange is

$$\langle \psi | R^2 | \psi \rangle = \frac{|\chi^\Gamma(a)|^2}{|\Gamma|^2} \quad (12)$$

where $\chi^\Gamma(a)$ is the character of any $a \in C_g$ for the representation Γ , i.e.,

$$\chi^\Gamma(a) = \text{Tr} [D^\Gamma(a)]. \quad (13)$$

Depending on the group, that probability can take values between 0 and 1. In the case where this probability

vanishes, it means that the charge has been transferred deterministically from the chargeon to the fluxon thanks to braiding, which is a very peculiar topological effect.

5. Dyon: anyon with nontrivial flux and nontrivial charge

While we have discussed how to label a chargeon (by an irrep) and a fluxon (by a conjugacy class), we have yet to discuss anyons that exhibit both a nontrivial charge and a nontrivial flux. Such an anyon is called a *dyon*. Suppose we wanted to measure the charge of a dyon. We could set up an interferometric experiment. We could place the dyon behind the slits in a double slit experiment and measure the interferometry pattern for any incoming test fluxon. However, since the dyon also carries flux, subtleties arise. Indeed, the passage of the test fluxon either to the left of the right of the dyon will modify the flux of the dyon. Thus, interference will only occur if the flux a of the dyon commutes with the flux b of the test fluxon, i.e., if $ab = ba$. In other words, the charge Γ of the dyon can be determined only if the probe fluxon has a flux among the elements b commuting with a , i.e., within the *normalizer* of a

Definition 2 (Normalizer).

$$\mathcal{N}_a = \{b \in G | ab = ba\}. \quad (14)$$

Note that a normalizer is always a subgroup of the group G . We thus conclude that the charge Γ of a dyon carrying flux a is not an irrep of the full G , but rather an irrep of the normalizer $\mathcal{N}(a)$.

The mathematical structure corresponding to an anyon model is the Drinfeld double of a group which is a quasi-triangular Hopf algebra. Anyon types are in one-to-one correspondence with the irreps of that operator algebra. Working out the irreps of the Drinfeld double only requires knowledge of the representation theory of the underlying group, since a key mathematical result is that irreps of a Drinfeld double are labelled by i) a conjugacy class and ii) an irrep of the normalizer of any element of the conjugacy class (which are all isomorphic).

6. Quantum dimension of an anyon

In a quantum double, the quantum dimension d_a associated to every anyon type a is the dimension of the vector subspace associated to that anyon. It is thus an integer. Given an anyon type (C_g, Γ) , its quantum dimension is

$$d_{(C_g, \Gamma)} = |C_g| |\Gamma|. \quad (15)$$

Moreover, another quantity of interest is the total quantum dimension \mathcal{D} of the model, which is related to the quantum dimension of every anyon type by

$$\mathcal{D}^2 = \sum_{\text{anyons } k} d_k^2. \quad (16)$$

In the case of a quantum double, the total quantum dimension is related to the cardinality of the group

$$\mathcal{D}^2 = |G|^2. \quad (17)$$

We will give an interpretation of this result in Sec. IV C.

At this point, we have defined anyons and described their braiding and fusion properties using a toy model of non-Abelian Aharonov-Bohm effect. We recovered, using a physics point of view, the key properties of the Drinfeld double of a group. However, in this toy model, anyons are fundamental particles and are put by hand. We will now describe the quantum double construction by Kitaev which allows to realize those anyons effectively as point-like excitations on a spin lattice.

B. Kitaev's quantum double on a lattice

A way to realize the non-abelian Aharonov-Bohm effect on a lattice is Kitaev's quantum double construction [1]. In this construction, charges reside on vertices and fluxes are on plaquettes of the lattice, however, fluxes and charges are not independent. A generic flux-charge composite particle (dyon) lives on a site: a combination of a vertex and a plaquette shown in Fig. 3.

This excitation structure is realized by first, assigning a Hilbert space to each edge of the lattice, the state of each edge can take any group element $z \in G$, then, defining a Hamiltonian that describes the interactions in this model. To introduce the Hamiltonian, let us define the following operators:

$$L_g^+ |z\rangle = |gz\rangle, \quad (18)$$

$$L_g^- |z\rangle = |zg^{-1}\rangle, \quad (19)$$

$$T_h^+ |z\rangle = \delta_{h,z} |z\rangle, \quad (20)$$

$$T_h^- |z\rangle = \delta_{h^{-1},z} |z\rangle, \quad (21)$$

where L_g^+ and L_g^- are the matrices representing left- and right-multiplication operators, T_h^+ and T_h^- are diagonal operators in the flux basis.

Then, we need to assign an orientation to the edges of the lattice. We use the convention shown in Fig. 3 for a site, i.e., the union of a vertex and a plaquette.

We now introduce two families of operators, following closely the original definition of [1].

Definition 3 (Plaquette operators). For any element $g \in G$, we define an operator acting on the 4 spins around a plaquette p

$$B_g^p = \sum_{h_1 h_2 h_3^{-1} h_4^{-1} = g} T_{h_1}^{+,1} \otimes T_{h_2}^{+,2} \otimes T_{h_3}^{-,3} \otimes T_{h_4}^{-,4} \quad (22)$$

where the use of T_h^+ vs. T_h^- depends on the orientation of the edge. One can easily see that with the T_h^+ , T_h^- projection operators acting on each edge, this operator indeed measures the full flux going through the plaquette.

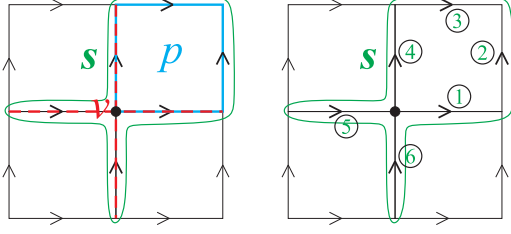


Figure 3. Our choice of orientation on the lattice, with (a) how a vertex and plaquette form a site, and (b) the edge numbering we used to define the vertex and plaquette operators \mathcal{A}_g^v and B_h .

Definition 4 (Vertex operators). For any element $g \in G$, we define a vertex operator, originally called star operators in [1], acting on the 4 spins around a vertex v

$$\mathcal{A}_g^v = L_g^{+,1} \otimes L_g^{+,4} \otimes L_g^{-,5} \otimes L_g^{-,6} \quad (23)$$

The projector unto the trivial flux at plaquette p is simply the plaquette operator for the trivial element B_e^p . The projector unto trivial charge A_1^v on vertex v is defined as

$$A_1^v = \sum_{g \in G} \mathcal{A}_g^v = \sum_{g \in G} L_g^{+,1} \otimes L_g^{+,4} \otimes L_g^{-,5} \otimes L_g^{-,6}, \quad (24)$$

where the use of L_g^+ vs. L_g^- again depends on the orientation of the edge with respect to the vertex. It is less trivial to see why this operator projects to the trivial charge: the trivial charge is labeled by the trivial representation of group G , and the 4-body vertex multiplication operators \mathcal{A}_g^v are summed up with equal weight, corresponding to the equal weight each group element has in the trivial representation.

How these operators act on a vertex and on a plaquette is illustrated in Fig. 4. In order for individual B_e^p to be properly defined even for a non-abelian group, we need to specify a starting vertex on the plaquette, then go around the edges of the plaquette in a counterclockwise manner. (This starting vertex is always marked with a black dot on the figures in this paper.) Whenever the orientation of an edge is opposite to this counterclockwise path B_h acts on it with T_h^- , otherwise it acts with T_h^+ . Similarly for the vertex operators: when the orientation of an edge points outwards from the vertex, \mathcal{A}_g^v acts with L_g^+ , otherwise with L_g^- .

Given vertex and plaquette operators, Kitaev introduced the following Hamiltonian in [1].

Definition 5 (Kitaev Hamiltonian). The Kitaev Hamiltonian of a quantum double $\mathcal{D}(G)$ is

$$H = - \sum_v A_1^v - \sum_p B_e^p, \quad (25)$$

Please note that Hamiltonian (25) assigns a extensive energy of -2 for every site in the vacuum (ground state),

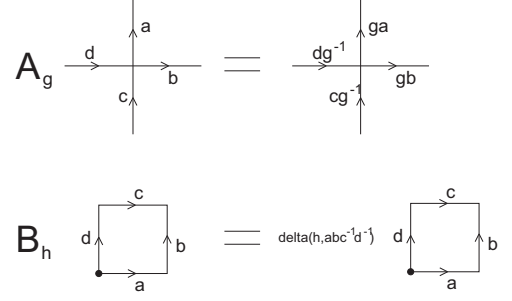


Figure 4. The effect of the individual projector terms (\mathcal{A}_g and B_h) on a vertex and on a plaquette, respectively.

a -1 energy to any pure charge or pure flux anyon, and a 0 energy to dyons.

1. Example: Toric code

The simplest example of the above quantum double construction is the toric code [1]. This is the quantum double of \mathbb{Z}_2 , thus the possible group elements on an edge can be: $\{0, 1\}$, and all additions are understood modulo 2: $0 \oplus 0 = 0$, $0 \oplus 1 = 1$, $1 \oplus 1 = 0$. The corresponding spin states $|0\rangle$ and $|1\rangle$ are the usual computational basis for qubits.

In \mathbb{Z}_2 , the left- and right-multiplication operators are the same: $L_0^+ = L_0^- = \mathbb{1}$ and $L_1^+ = L_1^- = X$, where X is the Pauli X operator. The diagonal operators are: $T_0^+ = T_0^- = (\mathbb{1} + Z)/2$ and $T_1^+ = T_1^- = (\mathbb{1} - Z)/2$, with Z being the Pauli Z operator.

The operators projecting unto trivial flux and trivial charge are (omitting the tensor product sign for simplicity): $A^v = I^1 I^4 I^5 I^6 + X^1 X^4 X^5 X^6$ and $B^p = I^1 I^2 I^3 I^4 + Z^1 Z^2 Z^3 Z^4$, thus the Hamiltonian is

$$H = - \sum_v (I^1 I^4 I^5 I^6 + X^1 X^4 X^5 X^6) - \sum_p (I^1 I^2 I^3 I^4 + Z^1 Z^2 Z^3 Z^4), \quad (26)$$

or in its widely known form, after redefining the ground state energy:

$$H = - \sum_v X^1 X^4 X^5 X^6 - \sum_p Z^1 Z^2 Z^3 Z^4. \quad (27)$$

Analyzing this Hamiltonian, we can see two main features of the model: i) the charges and fluxes have decoupled from each other which is typical of Abelian quantum double; ii) there is only one kind of excitation of either type (electric charge and magnetic flux) in this model. Therefore, in the toric code, the Kitaev Hamiltonian is a good description of both the vacuum and the excitations, even though the Hamiltonian only defines the vacuum projector; indeed, all that is not the vacuum can only be that one type of excitation.

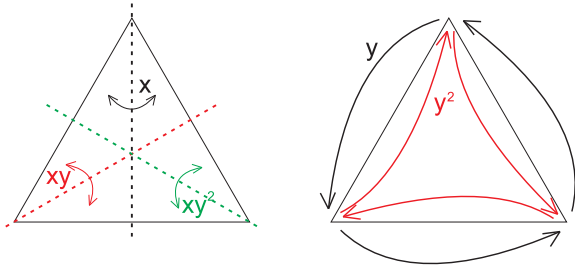


Figure 5. Symmetries of an equilateral triangle, or elements of the group S_3 .

2. Example of $\mathcal{D}(S_3)$

As a more elaborate example of the above quantum double structure, let's look at the quantum double of the smallest non-Abelian group, $\mathcal{D}(S_3)$. The group S_3 is isomorphic to the symmetry transformations of an equilateral triangle (see Fig. 5):

- identity: e ,
- rotations by $\pi/3$ and $2\pi/3$: y, y^2 ,
- mirrorings to the three different axes: x, xy, xy^2 .

Because of the nature of these symmetries: $y^3 = e$ and $x^2 = (xy)^2 = (xy^2)^2 = e$. The non-abelianity of S_3 is summed up by the commutation relation $xy = y^2x$.

The projectors projecting onto the trivial charge and flux in the specific example of $\mathcal{D}(S_3)$:

$$A_{(1)}^v = \mathcal{A}_e^s + \mathcal{A}_y^s + \mathcal{A}_{y^2}^s + \mathcal{A}_x^s + \mathcal{A}_{xy}^s + \mathcal{A}_{xy^2}^s, \quad (28)$$

$$B_{(e)}^p = \sum_{h_1 h_2 h_3^{-1} h_4^{-1} = e} T_{h_1}^{+,1} \otimes T_{h_2}^{+,2} \otimes T_{h_3}^{-,3} \otimes T_{h_4}^{-,4}, \quad (29)$$

examples of terms in the flux projector include, e.g. $T_e^{+,1} \otimes T_e^{+,2} \otimes T_e^{-,3} \otimes T_e^{-,4}$, $T_x^{+,1} \otimes T_x^{+,2} \otimes T_e^{-,3} \otimes T_e^{-,4}$, $T_{xy}^{+,1} \otimes T_{y^2}^{+,2} \otimes T_e^{-,3} \otimes T_x^{-,4}$, etc.

With these projectors the Hamiltonian is the same as the one introduced for a general G , see Eq. (25).

The anyon labels for this model are given by the conjugacy classes of S_3 and the irreducible representations of normalizers of conjugacy classes. There are three conjugacy classes of S_3 :

$$C_e = \{e\}, \quad (30)$$

$$C_y = \{y, y^2\}, \quad (31)$$

$$C_x = \{x, xy, xy^2\}, \quad (32)$$

and the corresponding normalizers are

$$N_e = S_3, \quad (33)$$

$$N_y = N_{y^2} = \{e, y, y^2\} \cong \mathbb{Z}_3, \quad (34)$$

$$N_x = \{e, x\} \cong N_{xy} \cong N_{xy^2} \cong \mathbb{Z}_2. \quad (35)$$

We would like to point out here that while the normalizers N_y and N_{y^2} are the same, independent of the

| S_3 | e | y | y^2 | x | xy | xy^2 |
|---------------------|--|--|--|--|--|--|
| $\Gamma_1^{S_3}$ | 1 | 1 | 1 | 1 | 1 | 1 |
| $\Gamma_{-1}^{S_3}$ | 1 | 1 | 1 | -1 | -1 | -1 |
| $\Gamma_2^{S_3}$ | $\begin{pmatrix} 1 & 0 \\ 0 & 1 \end{pmatrix}$ | $\begin{pmatrix} \bar{\omega} & 0 \\ 0 & \omega \end{pmatrix}$ | $\begin{pmatrix} \omega & 0 \\ 0 & \bar{\omega} \end{pmatrix}$ | $\begin{pmatrix} 0 & 1 \\ 1 & 0 \end{pmatrix}$ | $\begin{pmatrix} 0 & \omega \\ \bar{\omega} & 0 \end{pmatrix}$ | $\begin{pmatrix} 0 & \bar{\omega} \\ \omega & 0 \end{pmatrix}$ |

Table I. Irreducible representations of S_3 , i.e. the possible charge labels with flux C_e .

| \mathbb{Z}_3 | e | y | y^2 |
|--|-----|----------------|----------------|
| $\Gamma_1^{\mathbb{Z}_3}$ | 1 | 1 | 1 |
| $\Gamma_\omega^{\mathbb{Z}_3}$ | 1 | ω | $\bar{\omega}$ |
| $\Gamma_{\bar{\omega}}^{\mathbb{Z}_3}$ | 1 | $\bar{\omega}$ | ω |

| \mathbb{Z}_2 | e | x |
|------------------------------|-----|-----|
| $\Gamma_1^{\mathbb{Z}_2}$ | 1 | 1 |
| $\Gamma_{-1}^{\mathbb{Z}_2}$ | 1 | -1 |

Table II. Irreducible representations of (a) \mathbb{Z}_3 and (b) \mathbb{Z}_2 , i.e. the possible charge labels with flux C_x and C_y .

labeling, N_x , N_{xy} and N_{xy^2} are distinct, and only isomorphic to each other.

The irreducible representations of all these normalizers are listed in Tables I-II. There and in the remainder of the paper $\omega = \exp(2\pi i/3)$ and $\bar{\omega} = \exp(4\pi i/3)$ are the third complex roots of unity.

In summary, we have 8 anyons, these are listed in Table III. Anyon A is the vacuum since it has both trivial charge and flux. Anyons B and C are chargeons correspond respectively to the signed and two-dimensional irreps of S_3 . Anyons D and F are fluxons since they correspond to the trivial irrep of their respective normalizers. Other anyons are dyons.

Note, however, that in Table III anyons D and F have type "fluxon/dyon". Indeed, this feature will be important and will be explained more in detail in the next section. At this point, we only remark that it means that even in this model D and F might have either -1 or 0 mass, depending on whether they are $+1$ or 0 eigenstates of the A_v^1 projector. We will say that those anyons have two possible *flavors*.

| Label | C_g | N_g | Irrep. | Q.dim. | Type |
|-------|-------|----------------|-------------------------|--------|-------------|
| A | C_e | S_3 | Γ_1 | 1 | vacuum |
| B | C_e | S_3 | Γ_{-1} | 1 | chargeon |
| C | C_e | S_3 | Γ_2 | 2 | chargeon |
| D | C_x | \mathbb{Z}_2 | Γ_1 | 3 | fluxon/dyon |
| E | C_x | \mathbb{Z}_2 | Γ_{-1} | 3 | dyon |
| F | C_y | \mathbb{Z}_3 | Γ_1 | 2 | fluxon/dyon |
| G | C_y | \mathbb{Z}_2 | Γ_ω | 2 | dyon |
| H | C_y | \mathbb{Z}_2 | $\Gamma_{\bar{\omega}}$ | 2 | dyon |

Table III. Anyons of $\mathcal{D}(S_3)$ with their charge and flux labels, quantum dimensions and type.

III. TUNABLE QUANTUM DOUBLE HAMILTONIAN FOR ARBITRARY GROUP

We have seen in the previous section that in the case of the Kitaev Hamiltonian given by (25)) the energy spectrum is simple: the mass of an excitation is determined by its type (vacuum, charge, flux or dyon). It is then natural to wonder whether we can make the energy spectrum richer? Can we assign completely independent masses to the different anyons? And if yes, how will that change the excitation structure of the theory?

In this section, we introduce in Sec. III A a Hamiltonian that splits up the energies of different excitations for any quantum double, and then, in Sec. III B, work out explicitly the corresponding Hamiltonian for the quantum double of $\mathcal{D}(S_3)$.

A. Tunable quantum double construction

Our aim in this section is to introduce projectors unto different excitations. In Sec. II B we have already given the form of the trivial flux projector B_p and trivial charge projector A_s . Even though these vacuum projectors are independent of one another, and are both 4-body operators, it is not trivial that a projector unto an arbitrary excitation can be decomposed into independent 4-body charge- and flux-projectors. This is because, unlike in the case of abelian quantum doubles, the charge and flux of a site are tied to one another when considering dyons, i.e. the charge is defined as an irreducible representation of the normalizer of the flux conjugacy class.

This section is organized as follows. We will first comment on the reasons we insist on defining a Hamiltonian whose terms are four-body local in Sec. III A 1. We then outline our construction by recalling the definition of flux projectors and introducing novel charge projectors in Sec. III A 2. This allows us to define our tunable quantum double family of Hamiltonians in Sec. III A 3. Namely, Theorem 40 is the main result of this paper. In the following sections, we prove Theorem 40 by proving that the charge projectors are indeed an orthonormal family of projectors in Sec. III A 4 and then proving that they commute with the flux projectors in Sec. III A 5.

1. Locality of the Hamiltonian

A simple route to assign different masses to each anyon type would be to introduce a 6-local Hamiltonian. Indeed, each anyon lives on a site comprised of 6 spins. We can thus achieve the richest energy spectrum by introducing 6-local site projectors, projecting unto the different anyon species defined by the combination of a flux and a charge label, $P^s(C_h, \Gamma^{N_h})$. Then we can define a massive

Hamiltonian with these 6-local projectors:

$$H = \sum_s \sum_{C_h} \sum_{\Gamma^{N_h}} \alpha_{C_h, \Gamma^{N_h}}^s P^s(C_h, \Gamma^{N_h}), \quad (36)$$

and this way we can assign a different mass to each individual anyon.

There are mainly three reasons why we are not choosing to do this. First, we aim to have the non-abelian massive Hamiltonian be as close in form to the original Kitaev construction and the abelian generalization of [7], and we can achieve this without making our Hamiltonian more non-local. Second, our 4-local Hamiltonian does not break the quantum double structure, making it possible to understand the spectrum of excitations in terms of break up of representations of the group G into proper subgroups, see Sec. IV C. The third reason for 4-local terms in the Hamiltonian is that we have arguments that indicate that 2-local and 3-local Hamiltonians cannot be topological in 2D [13, 14] and we would like our Hamiltonian to remain local since it appears to be physically more realistic. Indeed, the 4-local toric code Hamiltonian can be recovered effectively in the right parameter regime of a nearest-neighbor 2-local, yet frustrated, Hamiltonian on a honeycomb lattice. More generally, there is a procedure to turn 4-local quantum double Hamiltonian for arbitrary group into a frustrated 2-local Hamiltonian thanks to a so-called 'gadget construction' [15]. Thus, minimizing the non-locality of the Hamiltonian is related to keeping it "physical".

2. Flux and charge projectors

The operators acting on a plaquette and projecting to a specific flux have already been introduced in Ref. [1]. They are straightforward generalization of plaquette operators. First, we define a new plaquette operator that requires the flux around the plaquette to be any group element g

$$B_h = \sum_{h_1 h_2 h_3^{-1} h_4^{-1} = h} T_{h_1}^+ \otimes T_{h_2}^+ \otimes T_{h_3}^- \otimes T_{h_4}^- \quad (37)$$

However, as pointed out earlier, a group element does not provide a gauge-invariant labelling of fluxons. Thus, we are lead to define a flux projector by considering a conjugacy class C_h

Definition 6 (Flux projectors). The flux projector associated to a conjugacy class C_h of a group G is

$$B_{C_h} = \sum_{h \in C_h} B_h. \quad (38)$$

We now introduce a novel family of projectors which generalizes the projector unto the trivial irrep introduced by Kitaev in [1]. Those *charge projectors* are cornerstones of our tunable quantum double construction.

Definition 7 (Charge projectors). The charge projector associated to an irreducible representation Γ of the group G is

$$A_\Gamma = \frac{d_\Gamma}{|G|} \sum_{g \in G} \chi_\Gamma(g) \mathcal{A}_g, \quad (39)$$

where d_Γ is the dimension of irrep Γ and $\chi_\Gamma(g) = \text{Tr}[\Gamma(g)]$ is the character of group element g in irrep Γ .

We defer the proof that those operators are indeed orthogonal projectors to Sec. III A 4. One can check that for abelian groups, our charge projectors reduce to those introduced in Refs. [7, 8]. Our charge projectors are reminiscent of similar objects introduced in [9, 16] using the representations themselves rather than the characters in the specific case of $D(S_3)$.

3. Definition of the tunable quantum double Hamiltonian

Having defined flux projectors by Eq. (38) and charge projectors by Eq. (39), we are now in position to our novel family of commuting Hamiltonians which assign different mass to different anyons.

Theorem 8. *The following family of topological Hamiltonian have commuting projector 4-local terms*

$$H = \sum_v \sum_{\text{irrep } \Gamma} \alpha_\Gamma A_\Gamma^v + \sum_p \sum_{C_g \subset G} \beta_{C_g} B_{C_g}^p \quad (40)$$

This family of commuting Hamiltonian is the central contribution of the paper. They are a new family of topological spin Hamiltonians made out a commuting projectors, similar to well-known families of topological models such as the Levin-Wen string-net models [17] and the Turaev-Viro codes [18]. Compared to Kitaev original quantum double Hamiltonians, they present the new feature of having tunable coupling constants that allow to assign different masses to anyons (although with some constraints) while preserving the useful mathematical properties of quantum doubles. Note that, for simplicity, we assumed the coupling coefficients to be independent of the vertices and the plaquettes although they need not be.

We will now prove in Sec. III A 4 that the operators defined by Eq. (39) are indeed projectors and then in Sec. III A 5 that the charge and the flux projectors are pairwise commuting.

4. Orthonormality of the charge projectors

Theorem 9 (Orthogonality of charge projectors). *The operators defined by Eq. (39) are orthonormal projectors*

$$A_\Gamma A_\Lambda = \delta_{\Gamma\Lambda} A_\Gamma \quad (41)$$

Theorem (9) is a non-trivial consequence of the Great Orthogonality Theorem (GOT), a strong result in representation theory which is usually stated at the level of matrix elements of two representations Γ and Λ of a group G [19].

Fact 10 (Great Orthogonality Theorem).

$$\sum_{g \in G} (\Gamma(g))_{ij} \overline{(\Lambda(g))_{i'j'}} = \frac{|G|}{d_\Gamma} \delta_{\Gamma\Lambda} \delta_{ii'} \delta_{jj'} \quad (42)$$

To prove Theorem 9, we first prove a basis-independent statement of the GOT (Lemma 11). To our knowledge, this operator restatement of the GOT is novel and could prove to be a useful tool in operator theory.

Lemma 11.

$$\sum_{g \in G} \Gamma(g) \otimes \Lambda(g^{-1}) = \frac{|G|}{d_\Gamma} \delta_{\Gamma\Lambda} S$$

where S is the swap operator, i.e., $S : \mathbb{C}^d \times \mathbb{C}^d \rightarrow \mathbb{C}^d \times \mathbb{C}^d$ is defined by $S(|i\rangle \otimes |j\rangle) = |j\rangle \otimes |i\rangle$.

Proof. The proof of Lemma (11) is a sequence of simplifications where the GOT is used to simplify Eq. (46):

$$\begin{aligned} & \sum_{g \in G} \Gamma(g) \otimes \Lambda(g^{-1}) \quad (43) \\ &= \sum_{g \in G} \sum_{ij} (\Gamma(g))_{ij} |i\rangle \langle j| \otimes \sum_{k\ell} (\Lambda(g^{-1}))_{k\ell} |k\rangle \langle \ell| \quad (44) \\ &= \sum_{g \in G} \sum_{ij} (\Gamma(g))_{ij} |i\rangle \langle j| \otimes \sum_{k\ell} \overline{(\Lambda(g))_{\ell k}} |k\rangle \langle \ell| \quad (45) \\ &= \sum_{ijk\ell} \sum_{g \in G} (\Gamma(g))_{ij} \overline{(\Lambda(g))_{\ell k}} |i\rangle \langle j| \otimes |k\rangle \langle \ell| \quad (46) \\ &= \sum_{ijk\ell} \frac{|G|}{d_\Gamma} \delta_{\Gamma\Lambda} \delta_{i\ell} \delta_{jk} |i\rangle \langle j| \otimes |k\rangle \langle \ell| \quad (47) \\ &= \frac{|G|}{d_\Gamma} \delta_{\Gamma\Lambda} \sum_{ij} |i\rangle \langle j| \otimes |j\rangle \langle i| \quad (48) \\ &= \frac{|G|}{d_\Gamma} \delta_{\Gamma\Lambda} S \quad (49) \end{aligned}$$

□

We can now prove Theorem 9.

Proof. Simple algebra shows that

$$A_s^\Gamma A_s^\Lambda = \frac{d_\Gamma d_\Lambda}{|G|^2} \sum_{g, g' \in G} \chi_\Gamma(g) \chi_\Lambda(g') A_s^g A_s^{g'} \quad (50)$$

$$= \frac{d_\Gamma d_\Lambda}{|G|^2} \sum_{h \in G} \underbrace{\sum_{g \in G} \chi_\Gamma(g) \chi_\Lambda(g^{-1}h)}_{(*)} A_s^h \quad (51)$$

We thus would like to prove that the $(*)$ term is proportionnal to $\delta_{\Gamma\Lambda} \chi_\Lambda(h)$.

Using the fact that $\text{Tr}[A \otimes B] = \text{Tr}[A] \text{Tr}[B]$, one can rewrite the (*) term as

$$(*) = \text{Tr} \left[\left(\sum_{g \in G} \Gamma(g) \otimes \Lambda(g)^\dagger \right) (\mathbb{I} \otimes \Lambda(h)) \right] \quad (52)$$

We can now use Lemma 11 to express the trace as

$$(*) = \delta_{\Gamma\Lambda} \frac{|G|}{d_\Gamma} \text{Tr} \left[\sum_{ij} |i\rangle\langle j| \otimes (|j\rangle\langle i|) \Lambda(h) \right] \quad (53)$$

$$= \delta_{\Gamma\Lambda} \frac{|G|}{d_\Gamma} \sum_{ij} \delta_{ij} \langle i | \Lambda(h) | j \rangle \quad (54)$$

$$= \delta_{\Gamma\Lambda} \frac{|G|}{d_\Gamma} \sum_i (\Lambda(h))_{ii} \quad (55)$$

$$= \delta_{\Gamma\Lambda} \frac{|G|}{d_\Gamma} \chi_\Lambda(h) \quad (56)$$

which concludes the proof of Theorem 9. \square

5. Commutation of flux/charge projectors

We now prove that the charge projectors defined by Eq. (38) and charge projectors defined by Eq. (39) are pairwise commuting. This commutation is key since it entails that the two families of projectors split the Hilbert space in a consistent way since states can be labelled by their common eigenstates.

Lemma 12 (Flux permutation by vertex operators). *For a plaquette p and vertex v that form a site, $(p, v) = s$*

$$B_g^{(p)} = \mathcal{A}_{h^{-1}}^{(v)} B_{hgh^{-1}}^{(p)} \mathcal{A}_h^{(v)}; \quad (57)$$

for a plaquette p and vertex v that are parts of different sites, $p \in s_1$, $v \in s_2$, $s_1 \neq s_2$

$$B_g^{(p)} = \mathcal{A}_{h^{-1}}^{(v)} B_g^{(p)} \mathcal{A}_h^{(v)}. \quad (58)$$

Proof. We will check the operator equality for an arbitrary state in which each spin is in a flux state (such states the full (Hilbert) space). Note that the plaquette operator B_g is in fact a projector unto states with flux g threading the plaquette while states having a different flux are annihilated by B_g . Thus, the Hilbert space is split into a direct sum

$$\mathcal{H} = I_g \oplus K_g \quad (59)$$

where I_g (resp. K_g) denotes the image (resp. kernel) of the projector. The image is spanned by states with flux g while states with other flux span the kernel. We will prove Eq. (57) first for a state in I_g and then for a state in K_g .

For a state $|\psi_g\rangle$ whose flux is g , i.e., $B_g|\psi_g\rangle = |\psi_g\rangle$ the application of the vertex operator \mathcal{A}_h will act non-trivially on two spins around the plaquette and change its

flux to hgh^{-1} (when the plaquette and vertex operators act on the same site, see Fig. 6). Thus, $\mathcal{A}_h|\psi_g\rangle$ is in the image of $B_{hgh^{-1}}$, i.e.,

$$\mathcal{A}_h|\psi_g\rangle = B_{hgh^{-1}}\mathcal{A}_h|\psi_g\rangle \quad (60)$$

Finally, applying $\mathcal{A}_{h^{-1}}$ will restore the spins into their original state and, in particular, restore the flux to $h^{-1}(hgh^{-1})h = g$, so that

$$\mathcal{A}_{h^{-1}}B_{hgh^{-1}}\mathcal{A}_h|\psi_g\rangle = |\psi_g\rangle. \quad (61)$$

Let's now consider a state $|\phi\rangle$ whose flux is not g , i.e., $B_g|\phi\rangle = 0$. That state is a linear combination of states with flux $f \neq g$. Let's assume that $|\phi\rangle$ has a well-defined flux f (the general case will follow by linearity). Then, $\mathcal{A}_h|\phi\rangle$ will have flux hfh^{-1} and will be annihilated by $B_{hgh^{-1}}$ since $hfh^{-1} \neq hgh^{-1}$. Thus,

$$\mathcal{A}_{h^{-1}}B_{hgh^{-1}}\mathcal{A}_h|\phi\rangle = 0. \quad (62)$$

Since we checked Eq. (57) on the two sectors of Eq. (59), it is valid for any state of the Hilbert space. Please note that we proved Eq. (57) only for one respective position of the vertex with respect to the plaquette. For the other three respective positions one can dutifully check that the proof is also valid, resulting in Eq. (58). \square

We now prove that vertex operators commute with flux projectors (although they do not commute with plaquette operators in general).

Theorem 13.

$$[B_{C_g}, \mathcal{A}_h] = 0 \quad (63)$$

Proof. Lemma 12 shows that the vertex operators \mathcal{A}_h map the states belonging to one flux sector to another flux sector. Note however that the new flux sector is in the same conjugacy class as the original flux. More formally, we have

$$\mathcal{A}_{h^{-1}}B_{C_g}\mathcal{A}_h = \sum_{f \in C_g} \mathcal{A}_{h^{-1}}B_f\mathcal{A}_h \quad (64)$$

$$= \sum_{f \in C_g} B_{h^{-1}fh} \quad (65)$$

$$= B_{C_g} \quad (66)$$

The commutation relation (63) follows by noting that $\mathcal{A}_{h^{-1}} = (\mathcal{A}_h)^{-1}$ since vertex operators are a representation of G . \square

The immediate corollary is that charge projectors also commute with flux projectors since they are linear combination of vertex operators.

Corollary 14.

$$[A_{\Gamma G}, B_{C_g}] = 0 \quad (67)$$

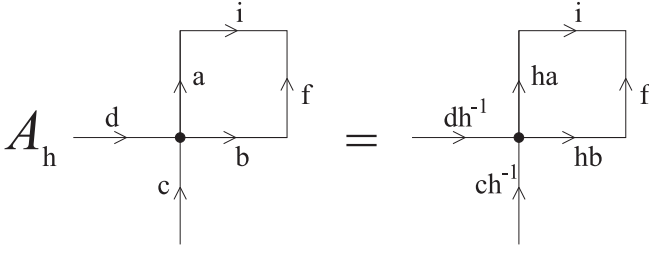


Figure 6. Relative configuration of a vertex and a plaquette in the case when the commutation of charge and flux projectors is nontrivial. The figure shows how a vertex operator acts on these spins. Note that the flux around the plaquette, starting from the vertex, is $g = bfi^{-1}a^{-1}$ prior to the application of A_h . Afterwards, the flux is now $g' = hbf i^{-1}(ha)^{-1} = hgh^{-1}$.

We can interpret the commutation of the 4-body projectors as a decoupling of the charges from the fluxes. However, there's an apparent catch with both this statement and this formalism: all the A_Γ charge projectors project unto an irreducible representation of the full group G , rather than the appropriate normalizer subgroups N_h to which the charges are actually assigned. So, how can we assign all different masses to the different anyons?

The answer is, we don't. We assign different weights to the different projector terms in the Hamiltonian, then determine the masses of the different anyons based on that. Some anyon masses will be related, some might even be the same. However, we will be able to tune every anyon mass, with the limitation that other anyon masses might change at the same time. Let's see how this manifests itself by working out in details the example of $\mathcal{D}(S_3)$.

B. Example of $\mathcal{D}(S_3)$

So how do we assign different masses to different anyons? Different flux classes can always be assigned masses different from each other, as the flux projectors are exact. These flux projectors in the case of $\mathcal{D}(S_3)$ are:

$$B_{C_e} = B_e, \quad (68)$$

$$B_{C_y} = B_y + B_{y^2}, \quad (69)$$

$$B_{C_x} = B_x + B_{xy} + B_{xy^2}, \quad (70)$$

and its trivial that by assigning weights to these terms in the Hamiltonian, masses of dyons with the same flux labels will also be affected.

The 4-body charge projectors for S_3 are:

$$A_{\Gamma_1} = \frac{1}{6}(\mathcal{A}_e + \mathcal{A}_y + \mathcal{A}_{y^2} + \mathcal{A}_x + \mathcal{A}_{xy} + \mathcal{A}_{xy^2}), \quad (71)$$

$$A_{\Gamma_{-1}} = \frac{1}{6}(\mathcal{A}_e + \mathcal{A}_y + \mathcal{A}_{y^2} - \mathcal{A}_x - \mathcal{A}_{xy} - \mathcal{A}_{xy^2}), \quad (72)$$

$$A_{\Gamma_2} = \frac{1}{3}(2\mathcal{A}_e - \mathcal{A}_y - \mathcal{A}_{y^2}), \quad (73)$$

| | Γ_1 | Γ_{-1} | Γ_2 |
|-------|------------|---------------|------------|
| C_e | A | B | C |
| C_x | D_1 | E_1 | D_2, E_2 |
| C_y | F_1 | F_2 | G, H |

Table IV. Split-up of anyons according to the 4-local charge- and flux projectors.

since they are based on the characters of the irreducible representations of S_3 . To determine whether dyons are affected by this assignment of masses, we point to the fact that the representations of S_3 and representations of its subgroups are related.

Specifically, assigning a weight to the term of trivial representation of S_3 (A_{Γ_1}) will affect both the vacuum (pure charge with trivial charge), and dyons D and F . This is because restricting the trivial representation of S_3 to the normalizer subgroup N_x or N_y will correspond to the trivial representation of both of those subgroups, thus to dyons D , F (please refer to Table III for anyon labels for S_3).

Similarly, if we assign a weight to the term of the alternating representation of S_3 , that will affect anyon B (chargeon), and dyons E and F . We can see that restricting the alternating representation of S_3 to N_x corresponds to the alternating representation of N_x (dyon E), and restricting it to N_y will give the trivial representation of N_y (dyon F).

Finally, tuning the weight of the two-dimensional representation of S_3 will affect chargeon C and dyons D , E and G , H . The two-dimensional representation, restricted to N_x or N_y will break up to two 1-dimensional representations on the subgroups. These 1-dimensional representations will be the trivial and the alternating of N_x (dyons D , E), and the two nontrivial representations of N_y (dyons G and H).

We refer the reader to Tables I-II to check these relations between the representations of S_3 and its subgroups. The result is the anyon masses in $\mathcal{D}(S_3)$ being related in the way shown in Table IV.

The massive Hamiltonian is then:

$$H = \sum_v (\alpha A_{\Gamma_1}^v + \beta A_{\Gamma_{-1}}^v + \gamma A_{\Gamma_2}^v) + \sum_p (\delta B_{C_e}^p + \epsilon B_{C_x}^p + \nu B_{C_y}^p), \quad (74)$$

and so this assigns the following masses to the anyons: $J_A = \alpha + \delta$, $J_B = \beta + \delta$, $J_C = \gamma + \delta$, $J_{D_1} = \alpha + \epsilon$, $J_{D_2} = \gamma + \epsilon$ (depending on the *flavor* of the particle), $J_{E_1} = \beta + \epsilon$ and $J_{E_2} = \gamma + \epsilon$, $J_{F_1} = \alpha + \nu$ and $J_{F_2} = \beta + \nu$, $J_G = \gamma + \nu$, $J_H = \gamma + \nu$, where the different masses assigned to the same anyon refer to that type of particle having different mass depending on its *flavor*.

In contrast, the 6-body projectors would have the form:

$$P_A = \frac{1}{6}(\mathcal{A}_e + \mathcal{A}_y + \mathcal{A}_{y^2} + \mathcal{A}_x + \mathcal{A}_{xy} + \mathcal{A}_{xy^2})B_{C_e} \quad (75)$$

$$P_B = \frac{1}{6}(\mathcal{A}_e + \mathcal{A}_y + \mathcal{A}_{y^2} - \mathcal{A}_x - \mathcal{A}_{xy} - \mathcal{A}_{xy^2})B_{C_e} \quad (76)$$

$$P_C = \frac{1}{3}(2\mathcal{A}_e - \mathcal{A}_y - \mathcal{A}_{y^2})B_{C_e}, \quad (77)$$

$$P_D = \frac{1}{2}(\mathcal{A}_e + \mathcal{A}_x)B_x + \frac{1}{2}(\mathcal{A}_e + \mathcal{A}_{xy})B_{xy} \\ + \frac{1}{2}(\mathcal{A}_e + \mathcal{A}_{xy^2})B_{xy^2}, \quad (78)$$

$$P_E = \frac{1}{2}(\mathcal{A}_e - \mathcal{A}_x)B_x + \frac{1}{2}(\mathcal{A}_e - \mathcal{A}_{xy})B_{xy} \\ + \frac{1}{2}(\mathcal{A}_e - \mathcal{A}_{xy^2})B_{xy^2}, \quad (79)$$

$$P_F = \frac{1}{3}(\mathcal{A}_e + \mathcal{A}_y + \mathcal{A}_{y^2})B_{C_y}, \quad (80)$$

$$P_G = \frac{1}{3}(\mathcal{A}_e + \omega\mathcal{A}_y + \bar{\omega}\mathcal{A}_{y^2})B_{C_y}, \quad (81)$$

$$P_H = \frac{1}{3}(\mathcal{A}_e + \bar{\omega}\mathcal{A}_y + \omega\mathcal{A}_{y^2})B_{C_y}. \quad (82)$$

Note that for anyon type D and E, the projectors are *not* a simple product of a projector acting on charges and a projector acting on flux (contrary to all other anyons of $\mathcal{D}(S_3)$). We call such anyons 'non-trivial dyons'. Those particles are more than the juxtaposition of a non-trivial charge and a non-trivial flux.

C. Case of an arbitrary quantum double $D(G)$

Taking a step back, a surprising feature of our tunable quantum double Hamiltonian is that irreps of normalizers that are proper subgroups of G do not have an associated Hamiltonian term. For instance, in the case of $\mathcal{D}(S_3)$, the irreps of \mathbb{Z}_2 and \mathbb{Z}_3 do not have an associated Hamiltonian term. How is it then that anyons D, E, F, G and H which are labelled by irreps of those two subgroups are correctly accounted for? The reason they have not been forgotten is that the irreps of those subgroups appear when restricting the irrep of S_3 to the fluxes within a normalizer. For instance, if we know that a dyon has flux in the conjugacy class C_y and that the charge on the vertex corresponds to the 2-dim irrep $\Gamma_2^{S_3}$, we should consider the action of this irrep restricted to the elements of the normalizer $\mathcal{N}(y)$. One can straightforwardly check that the 2-dim irrep of the group splits into two 1-dim irreps of the subgroup \mathbb{Z}_3 , i.e.,

$$\Gamma_2^{S_3}|_{\mathcal{N}(y)} = \Gamma_{\omega}^{\mathbb{Z}_3} \oplus \Gamma_{\bar{\omega}}^{\mathbb{Z}_3}. \quad (83)$$

Thus, the anyons $G = (C_y, \Gamma_{\omega}^{\mathbb{Z}_3})$ and $H = (C_y, \Gamma_{\bar{\omega}}^{\mathbb{Z}_3})$ are accounted for. However, our Hamiltonian will give them the same mass since it does not distinguish between them. This is a general feature of our construction in the sense that the splitting of irrep of the group G to recover irreps of the normalizer will happen for any group G .

Indeed, the statements about the correspondence between representations of the group and its subgroups can be made rigorous for any group G . For any finite group G when we assign the weight α_{Γ} to the A_{Γ} term, we give that mass to: the particle with trivial flux and Γ charge, as well as to all particles that have C_h flux and $\Gamma|_{N_h}$ charge, where C_h is any conjugacy class and $\Gamma|_{N_h}$ is the reduced representation of the Γ irrep. unto the subgroup N_h [19]. If $\Gamma|_{N_h}$ is reducible on N_h , then A_{Γ} will assign the same mass to all of the anyons corresponding to the irreducible components of $\Gamma|_{N_h}$. As mentioned in the previous paragraph, the coupling constant of the two-dim irrep. of S_3 will modify the mass of both G and H and also D and E .

Similarly, one might ask the question: if I take an anyon type randomly, does the 4-local Hamiltonian assign a non-zero mass to that? The answer is yes; if the anyon type is (C_h, Γ_h) , where Γ_h is an irrep. on the subgroup N_h , then we need to construct the induced representation from Γ_h on the full group G : $\text{Ind}_{N_h}^G(\Gamma_h)$ [19]. This will either be irreducible on G ($\text{Ind}_{N_h}^G(\Gamma_h) = \kappa$) thus correspond to the Hamiltonian term A_{κ} and mass α_{κ} is assigned to this anyon, or if the induced representation is reducible, the mass of the anyon will be the weight of one of the components, depending on the history of the anyon. Examples of the induced representation being irreducible itself are anyons G or H in the case of $\mathcal{D}(S_3)$, their labels are the nontrivial representations of N_y , and the induced representation is the 2-dimensional representation of S_3 in both cases. On the other hand, taking anyon F (e.g.), its label is the trivial representation of N_y , but the induced representation on S_3 is reducible: to the trivial and the alternating representations; thus the mass of F is modified by both tuning A_{Γ_1} and $A_{\Gamma_{-1}}$ in this example.

While the concept of representation splitting and induced representation might seem mathematical oddities, they will result in very interesting ways to split the Hilbert space, which we now discuss.

IV. HILBERT SPACE SPLITTING

In this Section, we elaborate on the way the charge and flux projectors split up the Hilbert space of a site. Indeed, we will see in Sec. IV A that each family of projectors provide a distinct way to split the Hilbert space unto which they are acting non-trivially. Moreover, since those projectors commute, those two splittings are consistent over the Hilbert space unto which they both act non-trivially, which has dimension $|G|^2$, as proven in Sec. IV B. Finally, in Sec. IV C, we introduce a diagrammatic representation of the splitting of that Hilbert that encapsulates all the results of this paper about the structure of tunable quantum double models.

A. Two distinct yet consistent ways to split the Hilbert space

We first prove that the charge and flux projectors, which respectively act non-trivially on four spins, add up to the identity operator on the Hilbert space of dimension $|G|^4$ of the four spins. Since they are orthogonal projectors, charge (resp. flux) projectors provide a orthogonal resolution of the identity, i.e., the direct sum of their images amounts to the full Hilbert space.

1. Resolution of the identity for charge projectors

Lemma 15. *The dimension of the image of the charge projector for the irreducible representation Γ is*

$$\text{Tr}[A^\Gamma] = |G|^3 d_\Gamma^2 \quad (84)$$

where d_Γ is the dimension of the irrep Γ .

Proof. Recall that the vertex operators \mathcal{A}_g are tensor product of 4 copies of the (left) regular representation L . $L(g)$ matrices are permutation with no fixed points, unless $g = e$. Since the trace of a tensor product is the product of the trace, $A(g)$ is traceless unless $g = e$. The vertex operator \mathcal{A}_e is nothing but the identity matrix on a space of dimension $|G|^4$. Thus,

$$\text{Tr}\mathcal{A}_g = |G|^4 \delta_{ge} \quad (85)$$

Simple calculation yields

$$\begin{aligned} \text{Tr}[A^\Gamma] &= \frac{d_\Gamma}{|G|} \sum_{g \in G} \chi_\Gamma(g) \text{Tr}\mathcal{A}_g \\ &= |G|^3 d_\Gamma \chi_\Gamma(e) \\ &= |G|^3 d_\Gamma^2 \end{aligned}$$

□

To see that the charge projectors add up to the identity on the Hilbert space of the 4 spins, we use a well-known fact from representation theory

$$\sum_{\Gamma} d_\Gamma^2 = |G|. \quad (86)$$

Dimension counting and the fact that charge projectors are orthogonal allows us to conclude that

$$\sum_{\Gamma} A^\Gamma = \mathbb{1}_{|G|^4} \quad (87)$$

i.e., the charge projectors are a orthogonal resolution of the identity for the Hilbert space of the 4 spins neighboring a vertex.

2. Resolution of the identity for flux projectors

Lemma 16. *The dimension of the image of the flux projector for the conjugacy class $C_g \subset G$ is*

$$\text{Tr}[B_{C_g}] = |C_g| |G|^3. \quad (88)$$

where $|C_g|$ is the cardinality of the conjugacy class.

Proof. Flux projectors are sum of rank-one projectors unto fluxes that belong to the same conjugacy class C_g . Thus, to compute the dimension of the image of the flux projectors, one needs to compute how many terms appear in the sum, i.e., how many ways 4 group elements can be multiplied such that their product belongs to the conjugacy class C_g . The first three group elements a, b, c can be chosen arbitrarily in $|G|^3$ distinct ways. Then the fourth group element d is chosen such that the product belongs to the conjugacy class C_g , i.e., $d \in (abc)^{-1}C_g$. Thus, there are $|C_g|$ choices for d . This concludes the proof. □

Moreover, since every group element belong to one and only one conjugacy class, we know that

$$\sum_{C_g \subset G} |C_g| = |G|. \quad (89)$$

Dimension counting and the fact that flux projectors are orthogonal allows us to conclude that

$$\sum_{C_g \subset G} B_{C_g} = \mathbb{1}_{|G|^4} \quad (90)$$

i.e., the flux projectors are a orthogonal resolution of the identity for the Hilbert space of the 4 spins of a plaquette.

B. Quantum dimension of a site

Since the flux and charge projectors pairwise commute (see Sec. III A 5), they provide consistent splitting of the Hilbert space unto which they both act non-trivially in the sense that a basis of this Hilbert space is spanned by common eigenstates. In this section, we work out the dimension of this common Hilbert space.

Recall that a site is the union of the four qudits around a plaquette and the four qudits around a neighboring vertex. Since 2 qudits are shared, a site consists of 6 qudits. However, each qudit belongs to three distinct sites: one site in which it belongs to both the vertex and the plaquette, one site for the other vertex and one site for the other plaquette, see Fig. 7. Thus, the quantum dimension assigned to every site is

$$d(\mathcal{H}_{\text{site}}) = \sqrt[3]{|G|^6} = |G|^2 \quad (91)$$

A simple way to think about it is that for every site, the two qudits shared between the vertex and the plaquette are assigned to this site while other qudits of the site are assigned to other neighboring sites.

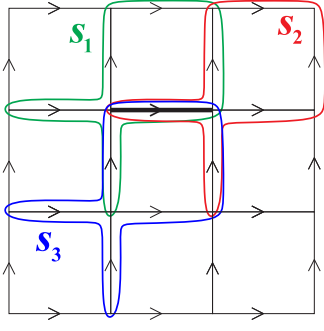


Figure 7. Illustration of the fact that every edge belongs to exactly 3 sites. For the thick edge in the figure the 3 sites are s_1 , s_2 and s_3 .

| | | $\Gamma_1^{S_3}$ | $\Gamma_{-1}^{S_3}$ | $\Gamma_2^{S_3}$ | |
|-------|--------|------------------|---------------------|------------------|-------|
| C_e | e | A | B | C | |
| | x | | | Dashed line | |
| C_x | xy | D_1 | E_1 | D_2 | E_2 |
| | xy^2 | | | Dashed line | |
| C_y | y | | | Dashed line | |
| | y^2 | F_1 | F_2 | G | H |

Figure 8. The flux and charge projectors of $\mathcal{D}(S_3)$ partition the Hilbert space of dimension $|S_3|^2 = 36$ unto which both family of operators act non-trivially. The charge projector splitting defines columns. The flux projectors, corresponding to conjugacy classes, define rows (each row between dotted lines corresponds to a group element). The 8 anyon types of $\mathcal{D}(S_3)$ are represented. Anyons D and E appear in two distinct flavors. Note that the area of the surface attributed to each anyon is equal to its quantum dimension. Dashed lines represent breaking-up of the two-dimensional irrep of S_3 over the normalizer of the group element of that row, see Eq. (92) and Eq. (93).

C. Diagrammatic representation

We now introduce a diagrammatic representation of the splitting of the Hilbert space of a site which we consider to be a very useful tool to better understand the structure of quantum double models.

The diagram, represented on Fig. 8 for the case of $\mathcal{D}(S_3)$, is a square of size $|G|$. Each column is indexed by an irrep Γ of G and its width is the squared dimension of the irrep d_Γ^2 . Similarly, each row is indexed by a conjugacy class C_g of G and its width is cardinality of the conjugacy class $|C_g|$.

Each intersection is now labelled by a conjugacy class

and an irrep. However, it does not correspond directly to an anyon type since an irrep of the full group G can split into the direct sum of irreps of the normalizer of the conjugacy class. For instance, in the case of $G = S_3$, the two-dimension irrep $\Gamma_2^{S_3}$ splits into two one-dimensional irrep of $\mathbb{Z}_3 \equiv \mathcal{N}(y) \equiv \mathcal{N}(y^2) = \{e, y, y^2\}$, i.e.,

$$\Gamma_2^{S_3}|_{\mathcal{N}(y)} = \Gamma_\omega^{\mathbb{Z}_3} \oplus \Gamma_{\bar{\omega}}^{\mathbb{Z}_3}. \quad (92)$$

This splitting defines anyon types G and H. We represent this splitting by drawing a dashed line. A similar splitting occurs when the two-dimensional irrep $\Gamma_2^{S_3}$ splits over the normalizer of C_x

$$\Gamma_2^{S_3}|_{\mathcal{N}(x)} = \Gamma_1^{\mathbb{Z}_2} \oplus \Gamma_{-1}^{\mathbb{Z}_2} \quad (93)$$

defining (parts) of the anyons D and E. Indeed, anyon D appears in two distinct rectangles of the diagram since the trivial irrep of \mathbb{Z}_2 can be obtained from the trivial irrep of S_3 or from the two-dimensional irrep of S_3 . We say that anyon D comes into two distinct *flavors*. D_1 has quantum dimension three and is within the image of the trivial irrep of S_3 whereas D_2 has quantum dimension six and is within the image of the two-dim irrep of S_3 . It might seem peculiar that a local observable allows to distinguish two subspace of internal states of anyon D . Note, however, that this feature is already present in the original quantum double construction since Kitaev's Hamiltonian would give different masses to D_1 which is a fluxon than D_2 which is a dyon (from the point of view of S_3). Similar properties hold for the two flavors of anyon E , labelled E_1 and E_2 , which would however not be distinguished by Kitaev's Hamiltonian.

Even in the smallest non-Abelian example of S_3 , irrep breaking leads to very intricate splitting of the Hilbert space. Consider the rectangle labelled by C_x and $\Gamma_2^{S_3}$. The two-dimensional irrep will split into the sum of two one-dimensional irrep of \mathbb{Z}_2 . However, the splitting is slightly different since the normalizers $\mathcal{N}_x, \mathcal{N}_{xy}$ and \mathcal{N}_{xy^2} , while isomorphic, are not equal. We indicate this on Fig. 8 by using three distinct dashed lines between the D_2 and E_2 rectangles.

Finally, note that the area of the rectangle (or the sum of the areas of distinct rectangles when an anyon has different flavors) is nothing but the squared quantum dimension of that anyon $(d_k)^2$. Since the area of the square is $|G|^2$, we recover the well-known result

$$\mathcal{D}^2 \equiv \sum_k (d_k)^2 = |G|^2 \quad (94)$$

This 'anyon splitting diagram' encapsulates most of the results of this paper. We hope this tool can be helpful to better understand the structure of the quantum double of a group G .

V. DISCUSSION

In this paper, we introduced a new family of 2D topological spin lattice models which generalize Kitaev's

quantum double construction. The Hamiltonian of this new class of topological models are given by a translation-invariant sum of local commuting terms acting each on 4 neighboring spins.

We provided a proof on the non-trivial commutation of those operators which is based on a basis-independent reformulation of the Great Orthogonality Theorem. Each local term can be multiplied by a coupling constant which makes the energy spectrum of those models richer than the original Kitaev quantum double construction. Moreover, we can tune the masses of the different anyons by modifying those coupling constants.

Tuning the masses of anyons will modify both the coherent dynamics and the incoherent dynamics of the topological model in the presence of a (thermal) environment. Thus, our family of Hamiltonian opens new possibility for quantum self-correcting models based on topological models. Indeed, our models generalize the Abelian construction of [7] where a parameter regime interesting for quantum self-correction was identified. In that regime, it was argued that entropic effects lead to a different scaling of the memory time. While that improvement was shown to not carry over in the low tem-

perature regime [8], a non-Abelian model might yield a different result or, at least, allow for a better understanding of entropic effects in quantum double models.

An interesting feature that arose out of our analysis was the definition of nontrivial dyons whose projector is not a simple product of a projector unto a charge by a projector unto a flux, see Sec. III B . We conjecture that any non-Abelian theory must exhibit at least one such non-trivial dyon.

VI. ACKNOWLEDGMENTS

We thank John Preskill, Alexei Kitaev, David Aasen, Ben Levitan and Sujeet Shukla for helpful discussions. We acknowledge funding provided by the Institute for Quantum Information and Matter, an NSF Physics Frontiers Center (NSF Grants PHY-1125565 and PHY-0803371) with support of the Gordon and Betty Moore Foundation (GBMF-12500028). OLC is partially supported by the Natural Sciences and Engineering Research Council of Canada (NSERC).

-
- [1] Alexei Kitaev. Fault-tolerant quantum computation by anyons. *Ann. Phys.*, 303(1):2–30, January 2003. ISSN 00034916. doi:10.1016/S0003-4916(02)00018-0.
 - [2] Sergey B Bravyi and A Yu Kitaev. Quantum codes on a lattice with boundary. *arXiv preprint quant-ph/9811052*, 1998.
 - [3] Austin G Fowler, Matteo Mariantoni, John M Martinis, and Andrew N Cleland. Surface codes: Towards practical large-scale quantum computation. *Physical Review A*, 86(3):032324, 2012.
 - [4] R Barends, J Kelly, A Megrant, A Veitia, D Sank, E Jeffrey, TC White, J Mutus, AG Fowler, B Campbell, et al. Superconducting quantum circuits at the surface code threshold for fault tolerance. *Nature*, 508(7497):500–503, 2014.
 - [5] AD Córcoles, Easwar Magesan, Srikanth J Srinivasan, Andrew W Cross, M Steffen, Jay M Gambetta, and Jerry M Chow. Demonstration of a quantum error detection code using a square lattice of four superconducting qubits. *Nature communications*, 6, 2015.
 - [6] Vladimir Gershonovich Drinfeld. Quantum groups. *Zapiski Nauchnykh Seminarov POMI*, 155:18–49, 1986.
 - [7] Benjamin J Brown, Abbas Al-Shimary, and Jiannis K Pachos. Entropic barriers for two-dimensional quantum memories. *Physical review letters*, 112(12):120503, 2014.
 - [8] Anna Kómár, Olivier Landon-Cardinal, and Kristan Temme. Necessity of an energy barrier for self-correction of abelian quantum doubles. *Physical Review A*, 93(5):052337, 2016.
 - [9] GK Brennen, Miguel Aguado, and J Ignacio Cirac. Simulations of quantum double models. *New Journal of Physics*, 11(5):053009, 2009.
 - [10] Salman Beigi, Peter W Shor, and Daniel Whalen. The quantum double model with boundary: condensations and symmetries. *Communications in mathematical physics*, 306(3):663–694, 2011.
 - [11] John Preskill. Lecture notes for physics 229: Quantum information and computation. *California Institute of Technology*, 1998.
 - [12] Parsa Hassan Bonderson. *Non-Abelian anyons and interferometry*. PhD thesis, California Institute of Technology, 2007.
 - [13] S. Bravyi and M. Vyalyi. Commutative version of the k-local hamiltonian problem and common eigenspace problem. *Quantum Inf. Comput.*, 5:187, 2005.
 - [14] Dorit Aharonov and Lior Eldar. On the complexity of commuting local hamiltonians, and tight conditions for topological order in such systems. In *Foundations of Computer Science (FOCS), 2011 IEEE 52nd Annual Symposium on*, pages 334–343. IEEE, 2011.
 - [15] Courtney G Brell, Steven T Flammia, Stephen D Bartlett, and Andrew C Doherty. Toric codes and quantum doubles from two-body hamiltonians. *New Journal of Physics*, 13(5):053039, 2011.
 - [16] James R Wootton, Jan Burri, Sofyan Iblisdir, and Daniel Loss. Error correction for non-abelian topological quantum computation. *Physical Review X*, 4(1):011051, 2014.
 - [17] Michael Levin and Xiao-Gang Wen. String-net condensation: A physical mechanism for topological phases. *Phys. Rev. B*, 71(4):1–21, January 2005. ISSN 1098-0121.
 - [18] Robert Koenig, Greg Kuperberg, and Ben W. Reichardt. Quantum computation with turaev-viro codes. *Annals of Physics*, 325(12):2707 – 2749, 2010. ISSN 0003-4916.
 - [19] Jean-Pierre Serre. *Linear representations of finite groups*, volume 42. Springer Science & Business Media, 2012.